


Local structure and ionic transport in acceptor-doped layered perovskite BaLa₂In₂O₇

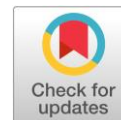
Nataliia A. Tarasova * 

Institute of High Temperature Electrochemistry of the Ural Branch of the Russian Academy of Sciences, Yekaterinburg 620990, Russia

* Corresponding author: natalia.tarasova@urfu.ru

This paper belongs to a Regular Issue.

© 2022, the Author. This article is published in open access under the terms and conditions of the Creative Commons Attribution (CC BY) license (<http://creativecommons.org/licenses/by/4.0/>).



Abstract

Materials with perovskite or perovskite-related structure have many applications because of their different physical and chemical properties. These applications are extremely diverse and cover different fields including hydrogen energy. Layered perovskites with Ruddlesden-Popper structure constitute a novel class of ionic conductors. In this paper, the effect of acceptor doping on the local structure and its relationship with transport properties were shown for layered perovskites based on BaLa₂In₂O₇ for the first time. The geometric factor (the increase in the unit cell volume due to the increase in the ionic radii of cations) plays a major role in the area of small dopant concentration ($x < 0.15$). The concentration factor (the increase in the oxygen vacancy concentration) is more significant in the area of big dopant concentration ($x > 0.15$). The acceptor doping is a promising way of improving the oxygen-ionic conductivity of layered perovskite BaLa₂In₂O₇.

Keywords

layered perovskite
ionic conductivity
acceptor doping
BaLa₂In₂O₇

Received: 11.10.22

Revised: 12.10.22

Accepted: 12.10.22

Available online: 19.10.22

1. Introduction

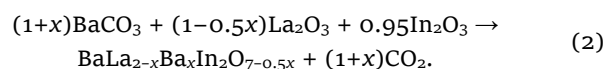
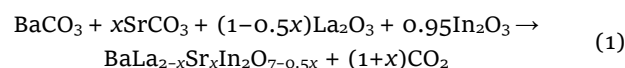
Materials with perovskite or perovskite-related structure have many applications because of their different physical and chemical properties. These applications are extremely diverse and cover fields from biomedical applications, including bone tissue engineering [1–5], to energetics, including hydrogen energy [6–10]. The perovskite structure has a high tolerance to various kinds of substitutions. However, a significant change in the sizes and charges of ions leads to a change in the structure to the perovskite-related structure. Layered perovskites represent one of the large classes of perovskite-related materials and include such structural classes as Ruddlesden-Popper [11, 12], Dion-Jacobson [13], and Aurivillius [14–16] structures. They can exhibit photocatalytic [17–19], ferroelectric [20–22], and luminescent [23–25] properties.

Several years ago, the possibility of ionic transport was revealed for the layered perovskites with the Ruddlesden-Popper structure [26]. Materials based on BaNdInO₄ [27–32], SrLaInO₄ [33–37], BaLaScO₄ [38], BaLaInO₄ [39–44], BaLa₂In₂O₇ [45, 46] and BaNd₂In₂O₇ [47, 48] were investigated as oxygen-ionic and protonic conductors. The effect of the doping on the local structure and its relationship with

transport properties was shown for layered perovskites based on BaLaInO₄ [49, 50]. In this paper, the local structure of acceptor-doped (Sr²⁺, Ba²⁺) layered perovskites based on BaLa₂In₂O₇ (Figure 1a) was investigated for the first time. The influence of geometric (dopant radius) and concentration (dopant concentration) factors on the ionic conductivity was revealed.

2. Experimental

The solid solutions BaLa_{2-x}Sr_xIn₂O_{7-0.5x} and BaLa_{2-x}Ba_xIn₂O_{7-0.5x} were obtained by a solid state method. The carbonates BaCO₃, SrCO₃ and the oxide In₂O₃ were initially dried and then weighed and mixed in stoichiometric quantities. The chemical reactions can be written as:



The reagents were milled in an agate mortar and then calcined at 800–1300 °C with the steps of 100 °C and the duration of calcination 24 h. The intermediate regrindings followed every heating step.

The Bruker Advance D8 diffractometer with Cu K α radiation was used for the monitoring of the phase purity of samples. The samples were prepared for XRD by heat treated at 1100 °C for 4 h and then cooled in dry Ar ($p_{\text{H}_2\text{O}} = 3.5 \cdot 10^{-5}$ atm). Ar atmosphere was used to avoid any carbonization of the samples.

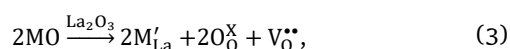
Raman spectra were collected on the modular confocal Raman microscopy system Alpha 300 AR (WiTec, Germany). The 10x objective lens (numerical aperture 0.2) were used to focus the blue laser ($\lambda = 488$ nm, 1800 g/mm exposure time 5 seconds, averaging three spectra) to a spot size around 3 μm . The spectral resolution was 1.22 cm^{-1} . The RayShield coupler with a specialized narrow band filter was used to cut off the Rayleigh scattering.

3. Results and Discussion

The homogeneity ranges of the solid solutions $\text{BaLa}_{2-x}\text{Sr}_x\text{In}_2\text{O}_{7-0.5x}$ and $\text{BaLa}_{2-x}\text{Ba}_x\text{In}_2\text{O}_{7-0.5x}$ were established using X-ray analysis. The compositions with $x \leq 0.2$ mol for $\text{BaLa}_{2-x}\text{Sr}_x\text{In}_2\text{O}_{7-0.5x}$ and $x \leq 0.3$ mol for $\text{BaLa}_{2-x}\text{Ba}_x\text{In}_2\text{O}_{7-0.5x}$ were single-phase. All samples belong to the $P4_2/\text{mmn}$ space group (tetragonal symmetry). Figure 1b represents the XRD patterns for Sr-doped composition $\text{BaLa}_{1.9}\text{Sr}_{0.1}\text{In}_2\text{O}_{6.95}$ as an example of the full-profile data fitting. The lattice parameters and unit cell volumes of doped compositions increased with increase in the dopant concentration (Figure 1c) because of the bigger ionic radii of the dopants ($r_{\text{La}^{3+}} = 1.216$ Å, $r_{\text{Sr}^{2+}} = 1.31$ Å, $r_{\text{Ba}^{2+}} = 1.47$ Å [51]). Local structure of the obtained compositions was investigated using the Raman spectroscopy method. The Raman spectra of solid solutions $\text{BaLa}_{2-x}\text{Ba}_x\text{In}_2\text{O}_{7-0.5x}$ and $\text{BaLa}_{2-x}\text{Sr}_x\text{In}_2\text{O}_{7-0.5x}$ are presented in Figures 2a and 2b, respectively.

The Raman spectra of all investigated compositions can be divided in two general regions. The first region includes the bending and stretching vibrations of polyhedra containing cations with bigger ionic radii (barium, strontium, lanthanum). This is a region of low, 120–200 cm^{-1} , wavenumbers. The modes ν_1 , ν_2 , ν_3 and ν_4 are observed in this region. They can be attributed to the M–O stretching and O–M–O bending vibrations of $[\text{BaO}_{12}]$ and $[\text{LaO}_9]$ polyhedra [49, 50, 52, 53]. The second region includes the tilting/bending and stretching vibrations of In-contained polyhedra and locates higher than 200 cm^{-1} wavenumbers. The tilting/bending vibrations of polyhedra $[\text{InO}_6]$ are described by the ν_5 , ν_6 , ν_7 , ν_8 , and ν_9 bands. The stretching vibrations of In-contained polyhedra should be located in the higher wavenumbers. The stretching vibrations of In–O bonds appear around 400 cm^{-1} for the monolayer perovskite BaLaInO_4 [49, 50]. The spectra of two-layer perovskites $\text{Sr}_{n+1}\text{TiInO}_{3n+1}$ [54] and $\text{Sr}_{n+1}\text{RuInO}_{3n+1}$ [55] contain two signals corresponding to the M–O stretching vibrations with lower and higher wavenumbers than the wavenumbers for their monolayer analogs. Based on this, ν_{10} , ν_{11} and ν_{12} bands can be assigned to In–O stretching vibrations.

Comparable analysis of the Raman spectra of solid solutions $\text{BaLa}_{2-x}\text{Ba}_x\text{In}_2\text{O}_{7-0.5x}$ and $\text{BaLa}_{2-x}\text{Sr}_x\text{In}_2\text{O}_{7-0.5x}$ show that they are all similar to each other. On the one hand, doping leads to the increase in the oxygen vacancy concentration in the crystal lattice:



where M'_{La} – Sr or Ba ions in La sites, $\text{V}_0^{\bullet\bullet}$ – an oxygen vacancy, O_0^{\times} – an oxygen atom in a regular position. Doping causes the decrease in the coordination number of metals.

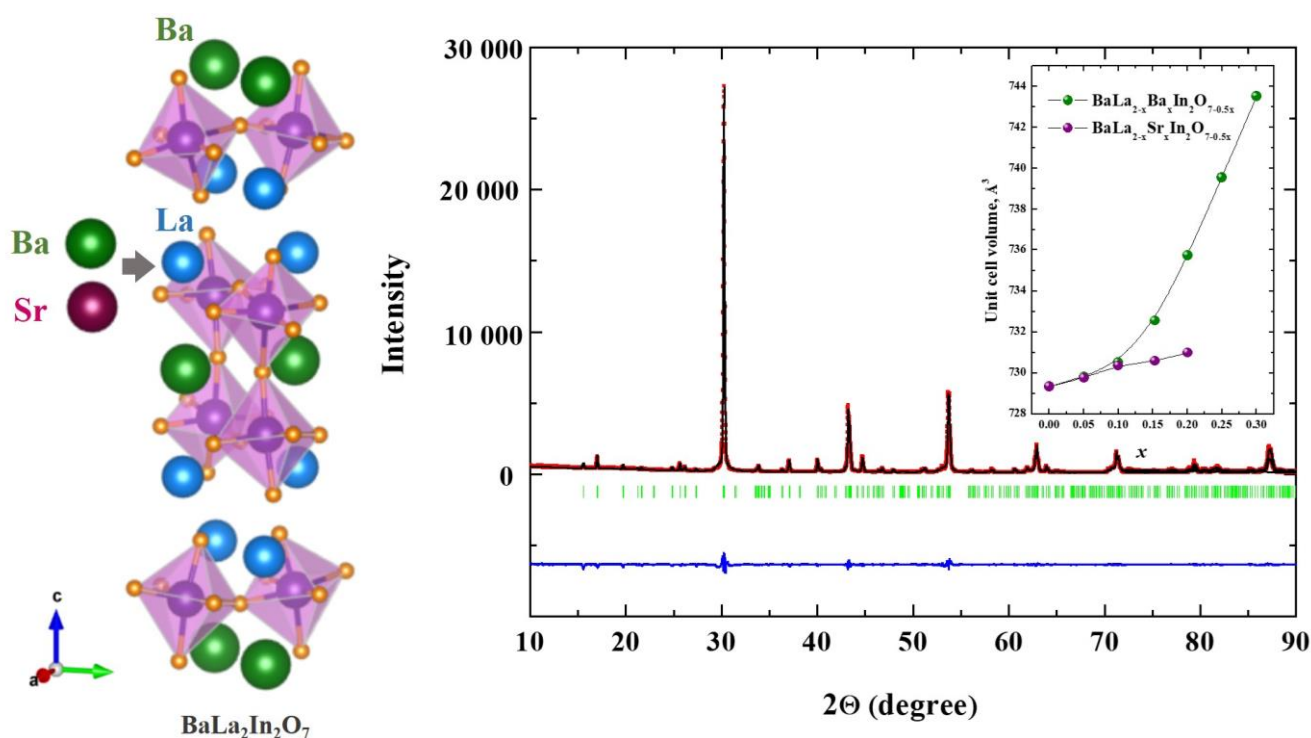


Figure 1 The scheme of acceptor doping of layered perovskite $\text{BaLa}_2\text{In}_2\text{O}_7$ (a), XRD patterns for the composition $\text{BaLa}_{1.9}\text{Sr}_{0.1}\text{In}_2\text{O}_{6.95}$ (b) and dependences of unit cell volume on dopant concentration for the solid solutions $\text{BaLa}_{2-x}\text{Sr}_x\text{In}_2\text{O}_{7-0.5x}$ and $\text{BaLa}_{2-x}\text{Ba}_x\text{In}_2\text{O}_{7-0.5x}$ (c).

Consequently, the bond length M–O should decrease in the vacancy-containing polyhedra, and the blue shift in the Raman spectra can be expected. On the other hand, doping by the ions with bigger ionic radii leads to the increase in the unit cell volume (Figure 1c) which could be due to increase of the bond length M–O. Based on this, the red shift in the Raman spectra can be expected. Obviously, the absence of significant shifts in the spectra of doped compositions is the resulting effect of the overlay of these processes (Figure 2). Meanwhile, the acceptor doping of layered perovskite BaLa₂In₂O₇ is accompanied by the changes in the ionic radii of cations (geometric factor) and the concentration of oxygen vacancies (concentration factor). Both of these factors should affect the ionic conductivity. It should be noted that the effect of acceptor doping on the local structure of monolayer perovskite BaLaInO₄ compared with that of the two-layer BaLa₂In₂O₇ perovskite was more pronounced [49, 50]. The monolayer perovskite structure contains the octahedra layers bonded only by axial oxygens and non-bonded by apical oxygens, in contrast with two-layer

structure where perovskite blocks contain the octahedrons connected by all six vertices. Obviously, the crystal lattice of a monolayer perovskite is more flexible and the changes in the local structure are more evident.

Figure 3 represents the dependences of oxygen-ionic conductivity and mobility for the solid solutions BaLa_{2-x}Ba_xIn₂O_{7-0.5x} and BaLa_{2-x}Sr_xIn₂O_{7-0.5x} obtained in the previous work [46]. As can be seen, the maximum in the conductivity and mobility curves is observed at a relatively small (0.1–0.15) dopant concentration. The most probable reason of oxygen mobility increasing in the area of small dopant concentration is the increase in the unit cell volume, i.e. in the space for ionic transfer in the crystal lattice. The presence of significant dopant concentration can lead to the formation of defect associates because of the interaction between defects with opposite charges:

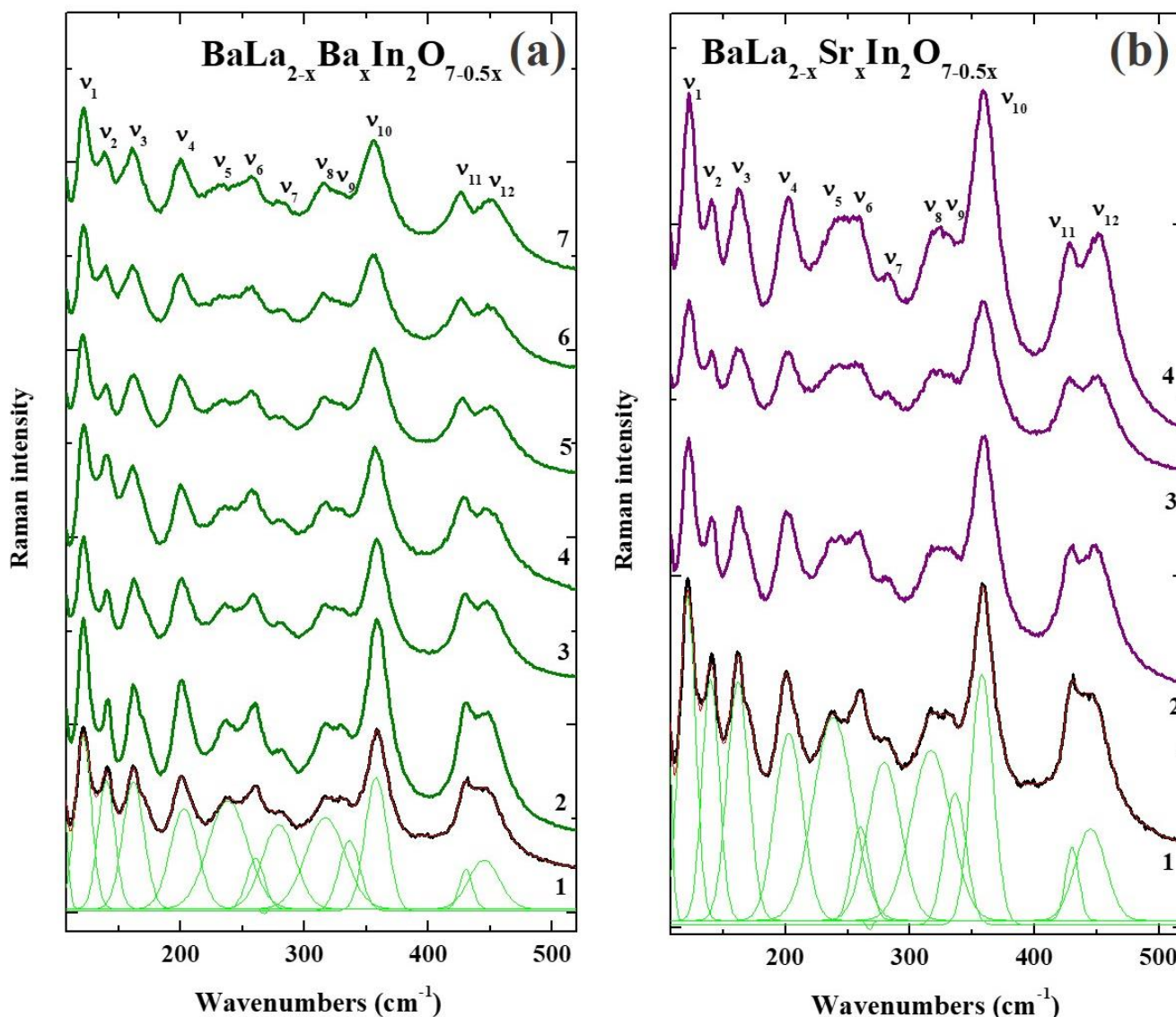
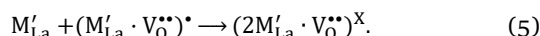
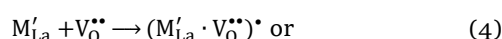


Figure 2 Raman spectra for the solid solutions BaLa_{2-x}Ba_xIn₂O_{7-0.5x} (a) and BaLa_{2-x}Sr_xIn₂O_{7-0.5x} (b).

Consequently, the oxygen mobility should decrease. As we can see (Figure 3), the decrease in the oxygen mobility determines the decrease in the oxygen conductivity despite the increase in the oxygen vacancy concentration and the increase in the unit cell volume.

Therefore, we can conclude, that ionic conduction in the acceptor-doped layered perovskite $\text{BaLa}_2\text{In}_2\text{O}_7$ is determined by several factors, including geometric (dopant radius) and concentration (dopant concentration) factors. The geometric factor (the increase in the unit cell volume due to the increase in the ionic radii of cations) plays major role in the area of small dopant concentration ($x < 0.15$). The concentration factor (the increase in the oxygen vacancy concentration) is more significant in the area of big dopant concentration ($x > 0.15$), where formation of defect associates is more probable.

4. Conclusions

In this paper, the local structure of solid solutions $\text{BaLa}_{2-x}\text{Ba}_x\text{In}_2\text{O}_{7-0.5x}$ and $\text{BaLa}_{2-x}\text{Sr}_x\text{In}_2\text{O}_{7-0.5x}$ was investigated. It was shown that several factors, including dopant radius and dopant concentration affect the changes in the oxygen ionic conductivity. The increase in the unit cell volume due to the increase in the ionic radii of cations (geometric factor) plays major role in the area of small dopant concentration ($x < 0.15$). The increase in the oxygen va-

cancy concentration (concentration factor) is more significant in the area of big dopant concentration ($x > 0.15$), where formation of defect associates is more probable. The acceptor doping is a promising way of improving the oxygen-ionic conductivity of layered perovskite $\text{BaLa}_2\text{In}_2\text{O}_7$.

Supplementary materials

Supplementary materials are available.

Funding

This research was performed according to the budgetary plan of the Institute of High Temperature Electrochemistry and funded by the Budget of Russian Federation

Acknowledgments

None.

Author contributions

Conceptualization: N.T.

Data curation: N.T.

Methodology: N.T.

Visualization: N.T.

Writing – original draft: N.T.

Writing – review & editing: N.T.

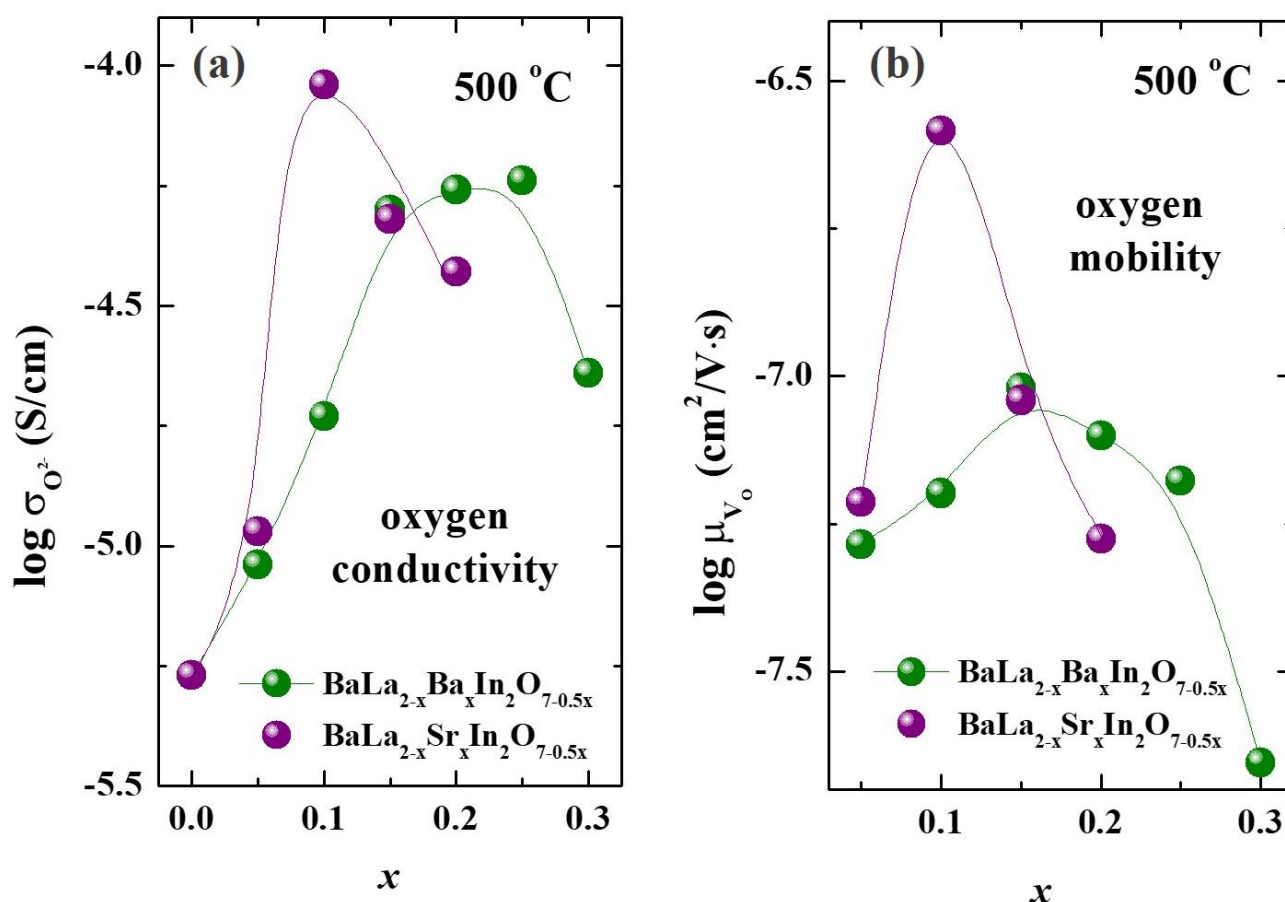


Figure 3 The concentration dependencies of oxygen-ionic conductivity (a) and mobility of oxygen ions (b) for the solid solutions $\text{BaLa}_{2-x}\text{Ba}_x\text{In}_2\text{O}_{7-0.5x}$ and $\text{BaLa}_{2-x}\text{Sr}_x\text{In}_2\text{O}_{7-0.5x}$.

Conflict of interest

The authors declare no conflict of interest.

Additional information

Author ID:

Natalia A. Tarasova, Scopus ID [37047923700](https://orcid.org/0009-0001-3704-7923).

Website:

Institute of High Temperature Electrochemistry UB RAS,
<http://www.ihte.uran.ru>.



References

- Punj P, Singh J, Singh K. Ceramic biomaterials: Properties, state of the art and future prospectives. *Ceram Int.* 2021;47:28059–28074. doi:[10.1016/j.ceramint.2021.06.238](https://doi.org/10.1016/j.ceramint.2021.06.238)
- Koons GL, Diba M, Mikos AG. Materials design for bone-tissue engineering. *Nature Rev Mater.* 2020;5:584–603. doi:[10.1038/s41578-020-0204-2](https://doi.org/10.1038/s41578-020-0204-2)
- Weng W, Wu W, Hou M, Liu T, Wang T, Yang H. Review of zirconia-based biomimetic scaffolds for bone tissue engineering. *J Mater Sci.* 2021;56:8309–8333. doi:[10.1007/s10853-021-05824-2](https://doi.org/10.1007/s10853-021-05824-2)
- Rosso JM, Volnistem EA, Santos IA, Bonadio TGM, Freitas VF. Lead-free NaNbO₃-based ferroelectric perovskites and their polar polymer-ceramic composites: Fundamentals and potentials for electronic and biomedical applications. *Ceram Int.* 2022;48:19527–19541. doi:[10.1016/j.ceramint.2022.04.089](https://doi.org/10.1016/j.ceramint.2022.04.089)
- Tarasova N, Galisheva A, Belova K, Mushnikova A, Volokitina E. Ceramic materials based on lanthanum zirconate for the bone augmentation purposes: materials science approach. *Chim Techn Acta.* 2022;9:20229209. doi:[10.15826/chimtech.2022.9.2.09](https://doi.org/10.15826/chimtech.2022.9.2.09)
- Duan C, Huang J, Sullivan N, O'Hayre R. Proton-conducting oxides for energy conversion and storage. *Appl Phys Rev.* 2022;7:011314. doi:[10.1063/1.5135319](https://doi.org/10.1063/1.5135319)
- Abdalla AM, Hossain S, Nisfindy OB, Azad AT, Dawood M, Azad AK. Hydrogen production, storage, transportation and key challenges with applications: A review. *Energy Convers Manag.* 2018;165:602–627. doi:[10.1016/j.enconman.2018.03.088](https://doi.org/10.1016/j.enconman.2018.03.088)
- Kim J, Sengodan S, Kim S, Kwon O, Bu Y, Kim G. Proton conducting oxides: A review of materials and applications for renewable energy conversion and storage. *Renewable and Sustainable.* *Energy Rev.* 2019;109:606–618. doi:[10.1016/j.rser.2019.04.042](https://doi.org/10.1016/j.rser.2019.04.042)
- Medvedev DA. Current drawbacks of proton-conducting ceramic materials: How to overcome them for real electrochemical purposes. *Curr Opin Green Sustain Chem.* 2021;32:100549. doi:[10.1016/j.cogsc.2021.100549](https://doi.org/10.1016/j.cogsc.2021.100549)
- Zvonareva I., Fu XZ, Medvedev D, Shao Z. Electrochemistry and energy conversion features of protonic ceramic cells with mixed ionic-electronic electrolytes. *Energy Environ. Sci.* 2021;15:439–465. doi:[10.1039/D1EE03109K](https://doi.org/10.1039/D1EE03109K)
- Ruddlesden SN, Popper P. New compounds of the K₂NiF₄ type. *Acta Cryst.* 1957;10:538–539. doi:[10.1107/S0365110X57001929](https://doi.org/10.1107/S0365110X57001929)
- Ruddlesden SN, Popper P. The compound Sr₃Ti₂O₇ and its structure. *Acta Cryst.* 1958;11:54–55. doi:[10.1107/S0365110X58000128](https://doi.org/10.1107/S0365110X58000128)
- Aurivillius B. Mixed Bismuth Oxides with Layer Lattices: I. Structure Type of CaBi₂B₂O₉. *Arkiv Kemi.* 1949;1:463–480.
- Dion M, Ganne M, Tournoux M. Nouvelles familles de phases M¹M²Nb₃O₁₀ a feuillets «perovskites». *Mat Res Bull.* 1981;16:1429–1435.
- Jacobson AJ, Lewandowski JT, Johnson JW. Ion exchange of the layered perovskite KCa₂Nb₃O₁₀ by protons. *J Less-Common Metal.* 1986;116:137–145.
- Jacobson AJ, Lewandowski JT, Johnson JW. Interlayer chemistry between thick transition-metal oxide layers: synthesis and intercalation reactions of K[Ca₂Na_{n-3}Nb_nO_{3n+1}]. *Inorg Chem.* 1985;24:3727–3729.
- Rodionov IA, Zvereva IA. Photocatalytic activity of layered perovskite-like oxides in practically valuable chemical reactions. *Russ Chem Rev.* 2016;85:248–85279. doi:[10.1070/RCR4547](https://doi.org/10.1070/RCR4547)
- Krashennnikova OV, Syrov EV, Smirnov SM, Suleimanov EV, Fukina DG, Knyazev AV, Titaev DN. Synthesis, crystal structure and photocatalytic activity of new Dion-Jacobson type titanoniobates. *J Solid State Chem.* 2022;315:123445. doi:[10.1016/j.jssc.2022.123445](https://doi.org/10.1016/j.jssc.2022.123445)
- Chawla H, Chandra A, Ingole P P, Garg S. Recent advancements in enhancement of photocatalytic activity using bismuth-based metal oxides Bi₂MO₆ (M = W, Mo, Cr) for environmental remediation and clean energy production. *J Ind Eng Chem.* 2021;95:1–15. doi:[10.1016/j.jiec.2020.12.028](https://doi.org/10.1016/j.jiec.2020.12.028)
- Ferreira WC, Rodrigues GLC, Araújo BS, de Aguiar FAA, de Abreu Silva, ANA, Fachine, PBA, de Araujo Paschoal CW; Ayala AP. Pressure-induced structural phase transitions in the multiferroic four-layer Aurivillius ceramic Bi₅FeTi₃O₁₅. *Ceram Int.* 2020; 46:18056–180621. doi:[10.1016/j.ceramint.2020.04.122](https://doi.org/10.1016/j.ceramint.2020.04.122)
- Zulhadjri Wendari TP, Ikhran M, Putri YE, Septiani U, Imelda. Enhanced dielectric and ferroelectric responses in La³⁺/Ti⁴⁺ co-substituted SrBi₂Ta₂O₉ Aurivillius phase. *Ceram Int.* 2022; 48:10328–103321. doi:[10.1016/j.ceramint.2022.01.307](https://doi.org/10.1016/j.ceramint.2022.01.307)
- Xu Q, Xie S, Wang F, Liu J, Shi J, Xing J, Chen Q, Zhu J, Wang Q. Bismuth titanate based piezoceramics: Structural evolutions and electrical behaviors at different sintering temperatures. *J Alloys Compd.* 2021;88215:160637. doi:[10.1016/j.jallcom.2021.160637](https://doi.org/10.1016/j.jallcom.2021.160637)
- Mamidi S, Gundeboina R, Kurra S, Velchuri R, Muga V. Aurivillius family of layered perovskites, BiREWO₆ (RE = La, Pr, Gd, and Dy): Synthesis, characterization, and photocatalytic studies. *Comptes Rendus Chimie.* 2018;21:547–552. doi:[10.1016/j.crci.2018.01.011](https://doi.org/10.1016/j.crci.2018.01.011)
- Zhou G, Jiang X, Zhao J, Molokeev M, Lin Z, Liu Q, Xia Z. Two-Dimensional-Layered Perovskite ALaTa₂O₇:Bi³⁺ (A = K and Na) Phosphors with Versatile Structures and Tunable Photoluminescence. *ACS Appl Mater Interfaces.* 2018;10:24648–246525. doi:[10.1021/acsami.8b08129](https://doi.org/10.1021/acsami.8b08129)
- Panda DP, Singh AK, Kundu TK, Sundaresan A. Visible-light excited polar Dion-Jacobson Rb(Bi_{1-x}Eu_x)₂Ti₂NbO₁₀ perovskites: Photoluminescence properties and in vitro bioimaging. *J Mater Chem. B* 2022;10:935–944. doi:[10.1039/d1tb02445k](https://doi.org/10.1039/d1tb02445k)
- Tarasova N, Animitsa I. A^{II}LnInO₄ with Ruddlesden-Popper structure for electrochemical applications: relationship between ion (oxygen-ion, proton) conductivity, water uptake and structural changes. *Mater.* 2022;15(1):114. doi:[10.3390/ma15010114](https://doi.org/10.3390/ma15010114)
- Ishigaki T, Hester JR. New perovskite-related structure family of oxide-ion conducting Materials NdBaInO₄. *Chem Mater.* 2014;26(8):2488–2491. doi:[10.1021/cm500776x](https://doi.org/10.1021/cm500776x)
- Fujii K, Shiraiwa M, Esaki Y, Yashima M, Kim SJ, Lee S. Improved oxide-ion conductivity of NdBaInO₄ by Sr doping. *J Mater Chem A.* 2015;3(22):11985–11990. doi:[10.1039/c5ta01336d](https://doi.org/10.1039/c5ta01336d)
- Ishihara T, Yan Y, Sakai T, Ida S. Oxide ion conductivity in doped NdBaInO₄. *Solid State Ion.* 2016;288:262–265. doi:[10.1016/j.ssi.2016.01.011](https://doi.org/10.1016/j.ssi.2016.01.011)
- Yang X, Liu S, Lu F, Xu J, Kuang X. Acceptor Doping and oxygen vacancy migration in layered perovskite NdBaInO₄-based

- mixed conductors. *J Phys Chem C*. 2016;12:6416–6426. doi:[10.1021/acs.jpcc.6b00700](https://doi.org/10.1021/acs.jpcc.6b00700)
31. Fujii K, Yashima M. Discovery and development of BaNdInO₄ – A brief review. *J Ceram Soc Japan*. 2018;126(10):852–859. doi:[10.2109/jcersj2.18110](https://doi.org/10.2109/jcersj2.18110)
 32. Zhou Y, Shiraiwa M, Nagao M, Fujii K, Tanaka I, Yashima M, Baque L, Basbus JF, Moggi LV, Skinner SJ. Protonic conduction in the BaNdInO₄ structure achieved by acceptor doping. *Chem Mater*. 2021;33(6):2139–2146. doi:[10.1021/acs.chemmater.0c04828](https://doi.org/10.1021/acs.chemmater.0c04828)
 33. Kato S, Ogasawara M, Sugai M, Nakata S. Synthesis and oxide ion conductivity of new layered perovskite La_{1-x}Sr_{1+x}InO_{4-d}. *Solid State Ion*. 2002;149(1–2):53–57. doi:[10.1016/S0167-2738\(02\)00138-8](https://doi.org/10.1016/S0167-2738(02)00138-8)
 34. Troncoso L, Alonso JA, Aguadero A. Low activation energies for interstitial oxygen conduction in the layered perovskites La_{1+x}Sr_{1-x}InO_{4+d}. *J Mater Chem A*. 2015;3(34):17797–17803. doi:[10.1039/c5ta03185k](https://doi.org/10.1039/c5ta03185k)
 35. Troncoso L, Alonso JA, Fernández-Díaz MT, Aguadero A. Introduction of interstitial oxygen atoms in the layered perovskite LaSrIn_{1-x}B_xO_{4+δ} system (B=Zr, Ti). *Solid State Ion*. 2015;282:82–87. doi:[10.1016/j.ssi.2015.09.014](https://doi.org/10.1016/j.ssi.2015.09.014)
 36. Troncoso L, Mariño C, Arce MD, Alonso JA. Dual oxygen defects in layered La_{1.2}Sr_{0.8-x}Ba_xInO_{4+d} (x = 0.2, 0.3) oxide-ion conductors: a neutron diffraction study. *Mater*. 2019;12(10):1624. doi:[10.3390/ma12101624](https://doi.org/10.3390/ma12101624)
 37. Troncoso L, Arce MD, Fernández-Díaz MT, Moggi LV, Alonso JA. Water insertion and combined interstitial-vacancy oxygen conduction in the layered perovskites La_{1.2}Sr_{0.8-x}Ba_xInO_{4+d}. *New J Chem*. 2019;43(15):6087–6094. doi:[10.1039/C8NJ05320K](https://doi.org/10.1039/C8NJ05320K)
 38. Shiraiwa M, Kido T, Fujii K, Yashima M. High-temperature proton conductors based on the (110) layered perovskite BaNdScO₄. *J Mat Chem A*. 2021;9:8607. doi:[10.1039/DoTA11573H](https://doi.org/10.1039/DoTA11573H)
 39. Tarasova N, Animitsa I, Galisheva A. Effect of acceptor and donor doping on the state of protons in block-layered structures based on BaLaInO₄. *Solid State Comm*. 2021;323:114093. doi:[10.1016/j.ssc.2020.114093](https://doi.org/10.1016/j.ssc.2020.114093)
 40. Tarasova N, Galisheva A, Animitsa I. Improvement of oxygen-ionic and protonic conductivity of BaLaInO₄ through Ti doping. *Ionics*. 2020;26:5075–5088. doi:[10.1007/s11581-020-03659-6](https://doi.org/10.1007/s11581-020-03659-6)
 41. Tarasova N, Galisheva A, Animitsa I. Ba²⁺/Ti⁴⁺- co-doped layered perovskite BaLaInO₄: the structure and ionic (O²⁻, H⁺) conductivity. *Int J Hydrog Energy*. 2021;46(32):16868–16877. doi:[10.1016/j.ijhydene.2021.02.044](https://doi.org/10.1016/j.ijhydene.2021.02.044)
 42. Tarasova N, Galisheva A, Animitsa I, Anokhina I, Gilev P, Cheremisina P. Novel mid-temperature Y³⁺ → In³⁺ doped proton conductors based on the layered perovskite BaLaInO₄. *Ceram Int*. 2022;48(11):15677–15685. doi:[10.1016/j.ceramint.2022.02.102](https://doi.org/10.1016/j.ceramint.2022.02.102)
 43. Tarasova N, Galisheva A, Animitsa I, Korona D, Davletbaev K. Novel proton-conducting layered perovskite based on BaLaInO₄ with two different cations in B-sublattice: Synthesis, hydration, ionic (O²⁻, H⁺) conductivity. *Int J Hydrog Energy*. 2022;47(44):18972–18982
 44. Tarasova N, Bedarkova A. Advanced proton-conducting ceramics based on layered perovskite BaLaInO₄ for energy conversion technologies and devices. *Mater*. 2022;15:6841. doi:[10.3390/ma15196841](https://doi.org/10.3390/ma15196841)
 45. Tarasova N, Galisheva A, Animitsa I, Korona D, Kreimesh H, Fedorova I. Protonic transport in layered perovskites BaLa_nIn_nO_{3n+1} (n = 1, 2) with Ruddlesden-Popper structure. *Appl Sci*. 2022;12(8):4082. doi:[10.3390/app12084082](https://doi.org/10.3390/app12084082)
 46. Tarasova N, Bedarkova A, Belova K, Abakumova E, Cheremisina P, Medvedev D. Oxygen ion and proton transport in alkali-earth doped layered perovskites based on BaLa₂In₂O₇. *Inorg*. 2022;10:161. doi:[10.3390/inorganics10100161](https://doi.org/10.3390/inorganics10100161)
 47. Tarasova N, Galisheva A, Animitsa I, Belova K, Egorova A, Abakumova E, Medvedev D. Layered Perovskites BaM₂In₂O₇ (M = La, Nd): From the Structure to the Ionic (O²⁻, H⁺) Conductivity. *Mater*. 2022;15:3488. doi:[10.3390/ma15103488](https://doi.org/10.3390/ma15103488)
 48. Tarasova N, Galisheva A. Phosphorus-doped protonic conductors based on BaLa_nIn_nO_{3n+1} (n = 1, 2): applying oxyanion doping strategy to the layered perovskite structures. *Chim Tehn Acta* 2022;9:20229405. doi:[10.15826/chimtech.2022.9.4.05](https://doi.org/10.15826/chimtech.2022.9.4.05)
 49. Tarasova N, Animitsa I, Galisheva A, Spectroscopic and transport properties of Ba- and Ti-doped BaLaInO₄. *J Raman Spec*. 2021;52:980–987. doi:[10.1002/jrs.6078](https://doi.org/10.1002/jrs.6078)
 50. Tarasova N, Animitsa I, Galisheva A, Effect of doping on the local structure of new block-layered proton conductors based on BaLaInO₄. *J Raman Spec*. 2021;51:2290–2297. doi:[10.1002/jrs.5966](https://doi.org/10.1002/jrs.5966)
 51. Shannon RD, Revised effective ionic radii and systematic studies of interatomic distances in halides and chalcogenides. *Acta Cryst*. 1976;A32:751–767. doi:[10.1107/S0567739476001551](https://doi.org/10.1107/S0567739476001551)
 52. Scherban T, Villeneuve R, Abello L, Lucazeau G. Raman scattering study of acceptor-doped BaCeO₃. *Solid State Ion*. 1993;61:93–98. doi:[10.1016/0167-2738\(93\)90339-5](https://doi.org/10.1016/0167-2738(93)90339-5)
 53. Chemarin C, Rosman N, Pagnier T, Lucazeau G. High-pressure raman study of mixed perovskites BaCe_xZr_{1-x}O₃ (0 ≤ x ≤ 1). *J Solid State Chem*. 2000;149:298–307. doi:[10.1006/jssc.1999.8530](https://doi.org/10.1006/jssc.1999.8530)
 54. Kamba S, SamoukPina F, Kadlec F, Pokorny J, Petzelt J, Reaney IM, Wise PL. Composition dependence of the lattice vibrations in Sr_{n+1}Ti_nO_{3n+1} Ruddlesden-Popper homologous series. *J Eur Ceram Soc*. 2003;23:2639–2645. doi:[10.1016/S0955-2219\(03\)00150-X](https://doi.org/10.1016/S0955-2219(03)00150-X)
 55. Iliev MN, Popov VN, Litvinchuk AP, Abrashev MV, Backstrom J, Sun YY, Mena RL, Chu CW. Comparative Raman studies of Sr₂RuO₄; Sr₃Ru₂O₇ and Sr₄Ru₃O₁₀. *Phys B*. 2005;358:138–152. doi:[10.1016/j.physb.2004.12.069](https://doi.org/10.1016/j.physb.2004.12.069)